Sectoral TFP News Shocks *

Appendix with supplementary material

Christoph Görtz
University of Birmingham

John D. Tsoukalas
University of Glasgow

March 2018

*Görtz: University of Birmingham, Department of Economics, Email: c.g.gortz@bham.ac.uk. Tsoukalas: University of Glasgow, Adam Smith Business School/Economics, Email: john.tsoukalas@glasgow.ac.uk.

A The VAR model

This section provides an overview about the underlying VAR model and the Minnesota prior used for the VAR coefficients. Consider the following reduced form VAR(p) model,

$$y_t = A(L)u_t,$$

where y_t is an $n \times 1$ vector of variables of interest, $A(L) = I + A_1 L + A_2 L^2 + ... + A_p L^p$ is a lag polynomial, $A_1, A_2, ..., A_p$ are $n \times n$ matrices of coefficients and, finally, u_t is an error term with $n \times n$ covariance matrix Σ. Define a linear mapping between reduced form, u_t, and structural errors, ε_t,

$$u_t = B_0 \varepsilon_t,$$

We can then write the structural moving average representation as

$$y_t = C(L)\varepsilon_t,$$

where $C(L) = A(L)B_0$, $\varepsilon_t = B_0^{-1}u_t$, and the matrix B_0 satisfies $B_0 B_0^{'} = \Sigma$. The B_0 matrix may also be written as $B_0 = \tilde{B}_0 D$, where $\tilde{B}_0$ is any arbitrary orthogonalization of Σ and D is an orthonormal matrix ($DD' = I$).

The h step ahead forecast error is,

$$y_{t+h} - E_{t-1}y_{t+h} = \sum_{\tau=0}^{h} A_\tau \tilde{B}_0 D \varepsilon_{t+h-\tau}.$$

The share of the forecast error variance of variable i attributable to shock j at horizon h is then

$$V_{i,j}(h) = \frac{e_i^{'}\Big(\sum_{\tau=0}^{h} A_\tau \tilde{B}_0 D e_j e_j^{'} D' \tilde{B}_0^{'} A_\tau^{'} \Big) e_i}{e_i^{'}\Big(\sum_{\tau=0}^{h} A_\tau \Sigma A_\tau^{'} \Big) e_i} = \frac{\sum_{\tau=0}^{h} A_{i,\tau} \tilde{B}_0 \gamma \gamma' \tilde{B}_0^{'} A_{i,\tau}^{'}}{\sum_{\tau=0}^{h} A_{i,\tau} \Sigma A_{i,\tau}^{'}},$$

where e_i denotes selection vectors with one in the i-th position and zeros elsewhere. The e_j vectors pick out the j-th column of D, denoted by γ. $\tilde{B}_0 \gamma$ is an $n \times 1$ vector corresponding to the j-th column of a possible orthogonalization and can be interpreted as an impulse response vector. In the following section, we discuss the estimation and identification methodology that yields an estimate for the TFP news shock from the VAR model.

We specify a Minnesota prior for the VAR coefficients, A, of the form

$$vec\,(A) \sim N\left(\underline{\beta}, \underline{V}\right),$$

where $\underline{\beta}$ is one for variables which are in log-levels, and zero for the corporate bond spread as well as inflation. The prior variance $\underline{V}$ is diagonal with elements,

$$\underline{V}_{i,jj} = \begin{cases} \frac{\underline{a}_1}{p^2} \text{ for coefficients on own lags} \\ \frac{\underline{a}_2 \sigma_{ii}}{p^2 \sigma_{jj}} \text{ for coefficients on lags of variable } j \neq i \\ \underline{a}_3 \sigma_{ii} \text{ for intercepts} \end{cases}$$

where, p denotes the number of lags. Here σ_{ii} is the residual variance from the unrestricted p-lag univariate autoregression for variable i. The degree of shrinkage depends on the hyperparameters $\underline{a}_1, \underline{a}_2, \underline{a}_3$. We set $\underline{a}_3 = 100$ and we select $\underline{a}_1, \underline{a}_2$ by searching on a grid and selecting the prior that maximizes the in-sample fit of the VAR, as measured by the Bayesian Information Criterion.[1]

B Robustness and Corroborative Results

B.1 Robustness to alternative identification approaches

In this section we show that our results are robust to alternative identification approaches used in the literature. These identification schemes have been proposed by Barsky and Sims (2011) and Forni et al. (2014) and are closely related to our baseline identification proposed by Francis et al. (2014) in that they all impose a zero impact restriction on TFP to identify the news shocks. The Barsky and Sims (2011) method identifies the news shock as the shock that maximizes the forecast error variance over a horizon from zero to forty quarters. Forni et al. (2014) identify the news shock as the shock that has maximum impact on TFP at the forty quarter horizon. We prefer the Max Share method of Francis et al. (2014), compared to the closely related Barsky and Sims (2011) method, since the latter seeks the shock that maximizes the FEV of TFP at long and short horizons, potentially confounding temporary and permanent future TFP shocks. In addition, revisions in utilization estimates in successive revisions of the TFP data can be a source of short run measurement error; the Max Share method by the nature of the maximization problem, is preferable compared to the Barsky and Sims (2011) method, which may not be robust to this source of measurement error. The advantage of the Max Share method over the Forni et al. (2014) method is that the former treats the maximization horizon as a parameter that the user can change.

[1]The grid of values we use is:
$\underline{a}_1$ = (1e-5,2e-5,3e-5,4e-5,5e-5,6e-5,7e-5,8e-5,9e-5, 1e-4,2e-4,3e-4,4e-4,5e-4,6e-4,7e-4,8e-4,9e-4, 0.001,0.002,0.003,0.004,0.005,0.006,0.007,0.008,0.009, 0.01,0.02,0.03,0.04,0.05,0.06,0.07,0.08,0.09, 0.1,0.2,0.3,0.4,0.5,0.6,0.7,0.8,0.9, 1,2,3,4,5,6,7,8,9,10),
$\underline{a}_2$ = (0.01,0.02,0.03,0.04,0.05,0.06,0.07,0.08,0.09, 0.1,0.2,0.3,0.4,0.5,0.6,0.7,0.8,0.9,1,2,3,4,5,6,7,8,910).
We take all possible pairs of $\underline{a}_1$ and $\underline{a}_2$ in the above grids, so we end up estimating 1540 models.

Figures 1, 2 and 3 display the median IRFs for VAR specification II. It is evident that these are virtually indistinguishable for either the aggregate or the two sectoral TFP news shocks.

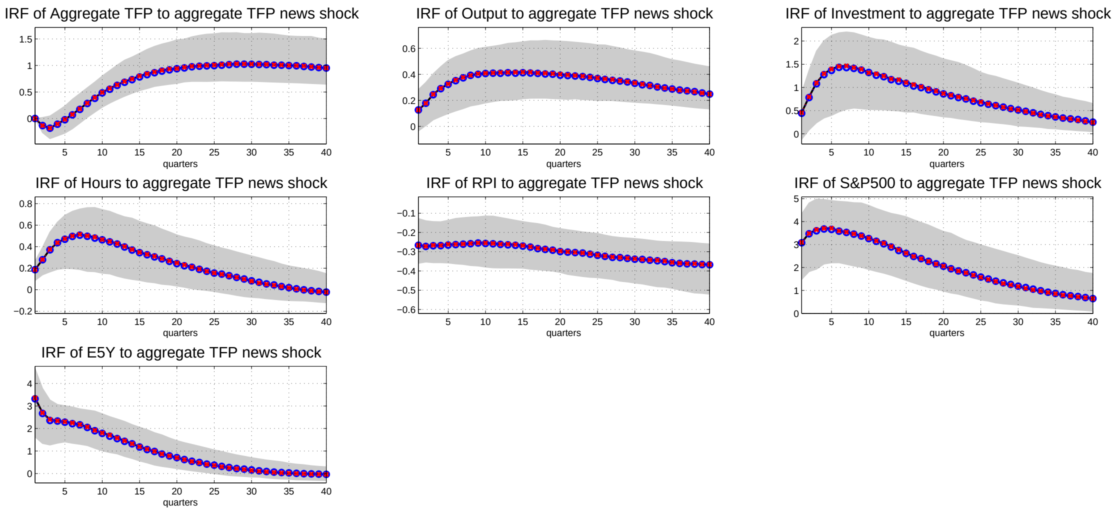

Figure 1: **Aggregate TFP news shock, specification II.** Median responses to a aggregate TFP news shock identified using the baseline scheme proposed by Francis et al. (2014) (black solid line), the Barsky and Sims (2011) methodology (red line with crosses) and the Forni et al. (2014) methodology (blue line with circles). The shaded gray areas are the 16% and 84% posterior bands generated from the posterior distribution of VAR parameters corresponding to the baseline identification. The units of the vertical axes are percentage deviations.

B.2 Robustness to horizon of variance maximization in shock identification

In the main body of the paper the Max Share methodology identifies the news shock as the shock that (i) does not move TFP on impact and (ii) maximizes the variance of TFP at a specific finite horizon. As a baseline specification in the paper we have set the horizon to 40 quarters which is the baseline specification used in several existing papers in the literature, e.g. Barsky and Sims (2011). Figures 4, 5 and 6 show that our results are also robust to varying this horizon to 30 or 50 quarters.

B.3 Robustness to the number of lags

We undertake robustness tests also with respect to the number of lags used in the VAR. Figures 7, 8 and 9 show that the baseline specification with three lags delivers very similar results to specifications with four or five lags.

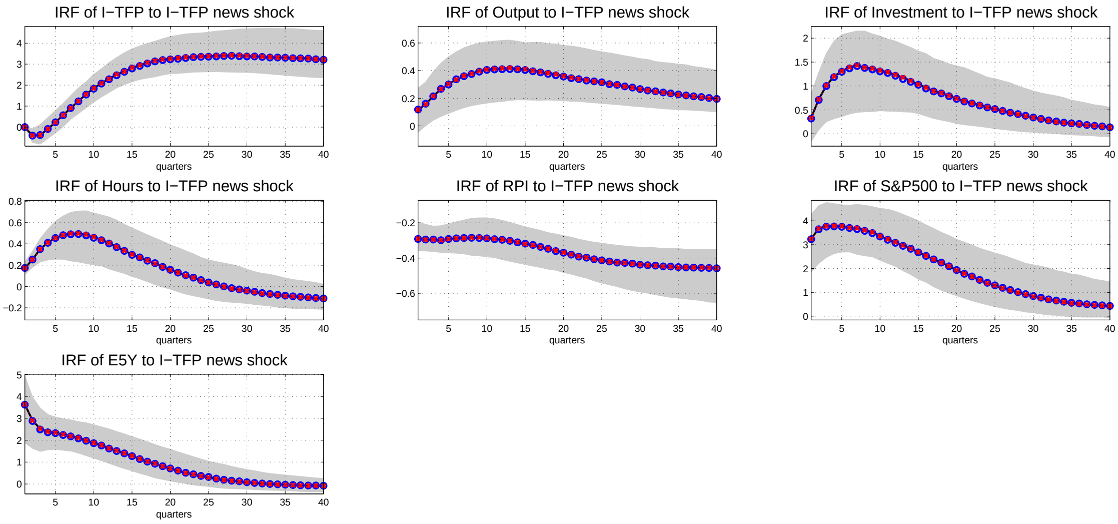

Figure 2: **Investment specific TFP news shock, specification II.** Median responses to a investment sector TFP news shock identified using the baseline scheme proposed by Francis et al. (2014) (black solid line), the Barsky and Sims (2011) methodology (red line with crosses) and the Forni et al. (2014) methodology (blue line with circles). The shaded gray areas are the 16% and 84% posterior bands generated from the posterior distribution of VAR parameters corresponding to the baseline identification. The units of the vertical axes are percentage deviations.

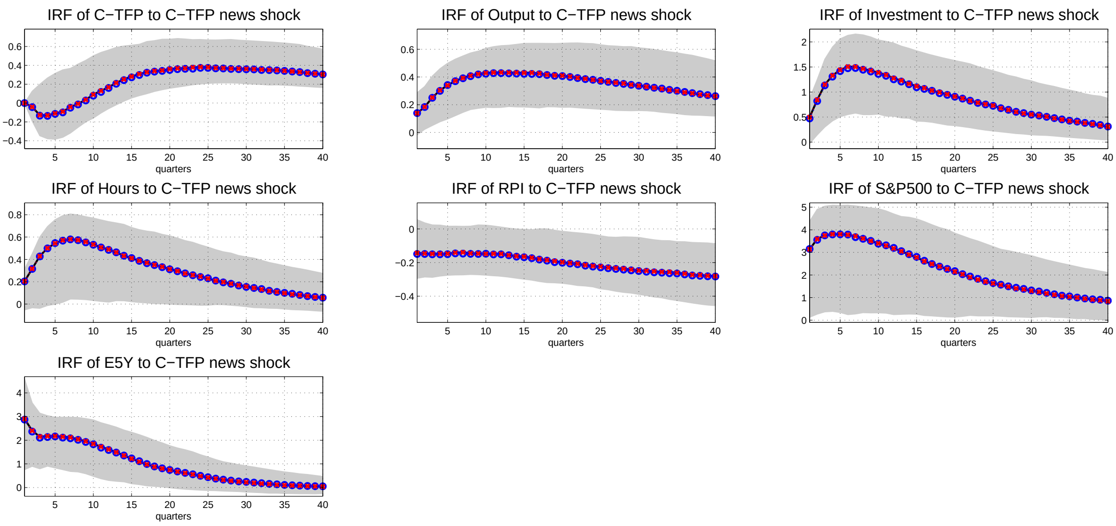

Figure 3: **Consumption specific TFP news shock, specification II.** Median responses to a consumption sector TFP news shock identified using the baseline scheme proposed by Francis et al. (2014) (black solid line), the Barsky and Sims (2011) methodology (red line with crosses) and the Forni et al. (2014) methodology (blue line with circles). The shaded gray areas are the 16% and 84% posterior bands generated from the posterior distribution of VAR parameters corresponding to the baseline identification. The units of the vertical axes are percentage deviations.

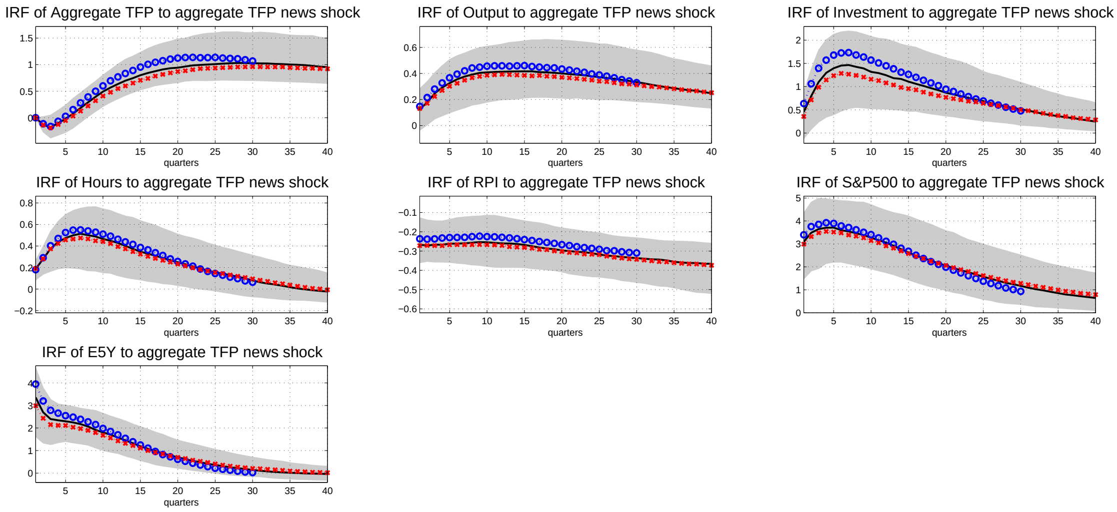

Figure 4: **Aggregate TFP news shock, specification II.** Median responses to a aggregate TFP news shock using a 40 quarter horizon (black solid line), 50 quarter horizon (red line with crosses) and 30 quarter horizon (blue line with circles). The shaded gray areas are the 16% and 84% posterior bands generated from the posterior distribution of VAR parameters corresponding to the baseline identification with three lags. The units of the vertical axes are percentage deviations.

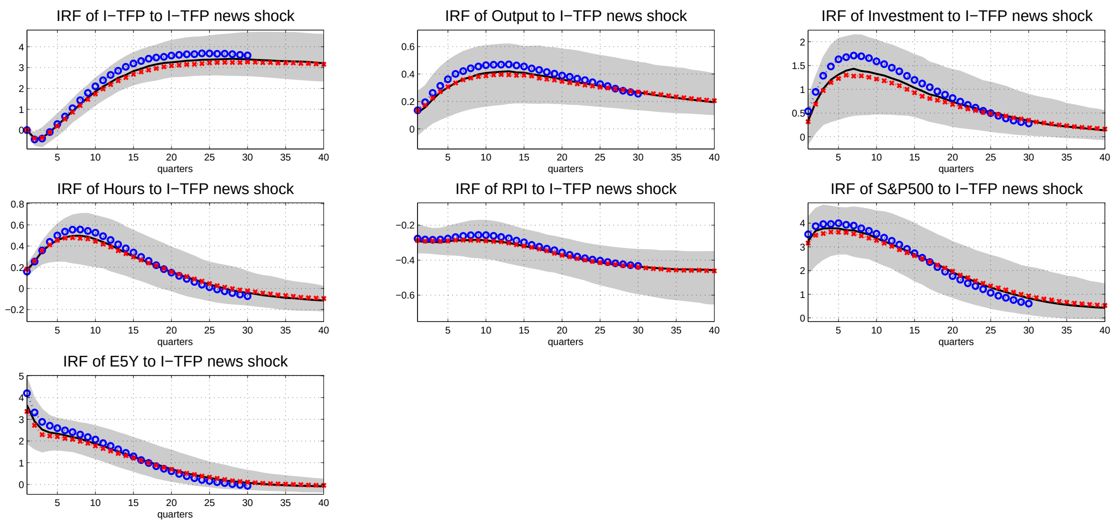

Figure 5: **Investment specific TFP news shock, specification II.** Median responses to a investment sector TFP news shock using a 40 quarter horizon (black solid line), 50 quarter horizon (red line with crosses) and 30 quarter horizon (blue line with circles). The shaded gray areas are the 16% and 84% posterior bands generated from the posterior distribution of VAR parameters corresponding to the baseline identification with three lags. The units of the vertical axes are percentage deviations.

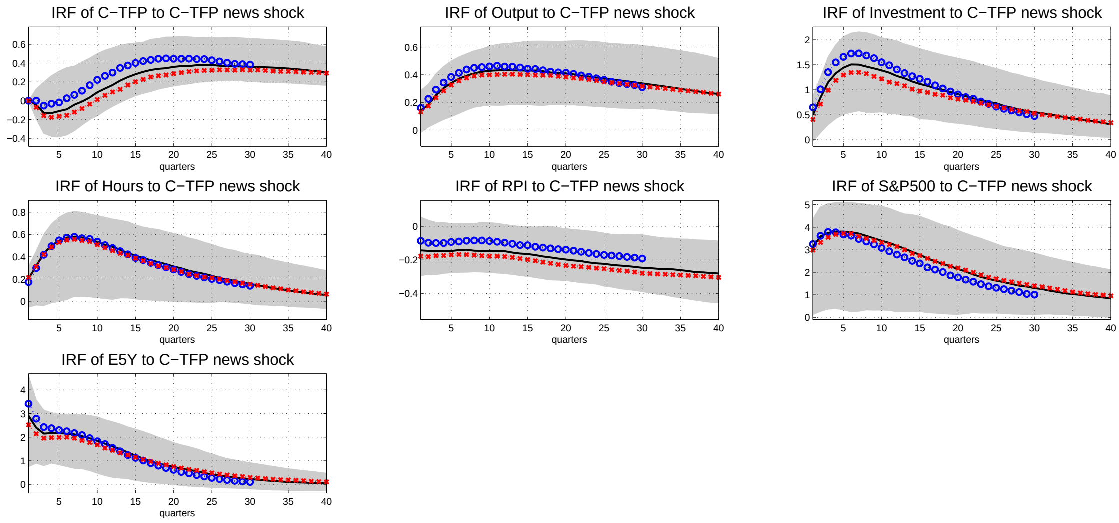

Figure 6: **Consumption specific TFP news shock, specification II.** Median responses to a consumption sector TFP news shock using a 40 quarter horizon (black solid line), 50 quarter horizon (red line with crosses) and 30 quarter horizon (blue line with circles). The shaded gray areas are the 16% and 84% posterior bands generated from the posterior distribution of VAR parameters corresponding to the baseline identification with three lags. The units of the vertical axes are percentage deviations.

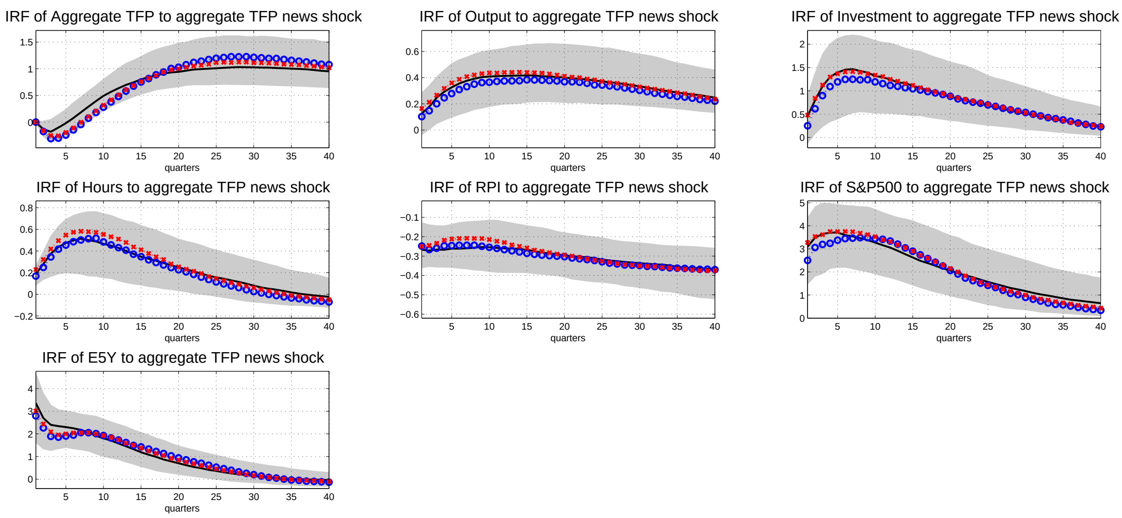

Figure 7: **Aggregate TFP news shock, specification II.** Median responses to a aggregate TFP news shock using three lag (black solid line), four lags (red line with crosses) and five lags (blue line with circles). The shaded gray areas are the 16% and 84% posterior bands generated from the posterior distribution of VAR parameters corresponding to the baseline identification with three lags. The units of the vertical axes are percentage deviations.

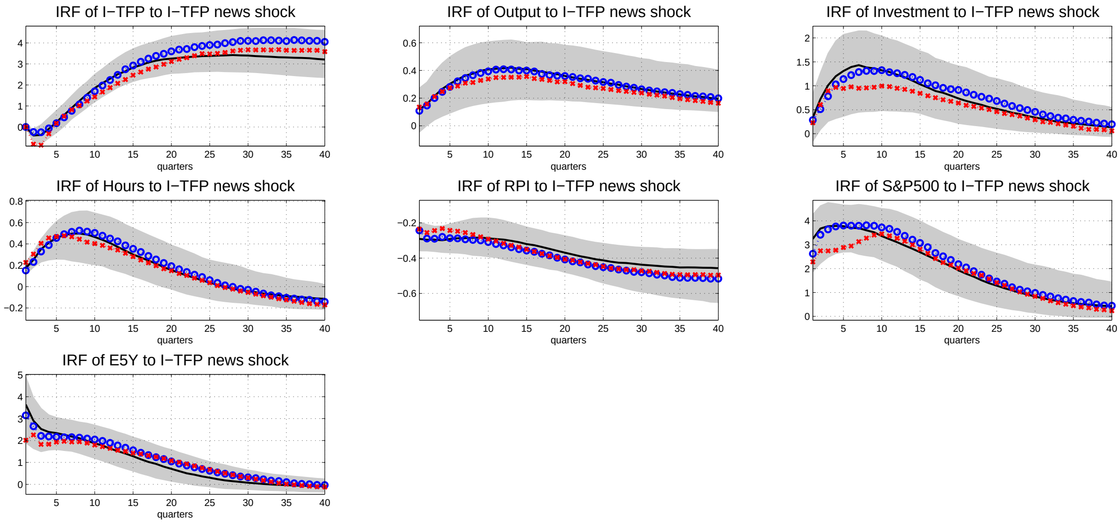

Figure 8: **Investment specific TFP news shock, specification II.** Median responses to a investment sector TFP news shock using three lag (black solid line), four lags (red line with crosses) and five lags (blue line with circles). The shaded gray areas are the 16% and 84% posterior bands generated from the posterior distribution of VAR parameters corresponding to the baseline identification with three lags. The units of the vertical axes are percentage deviations.

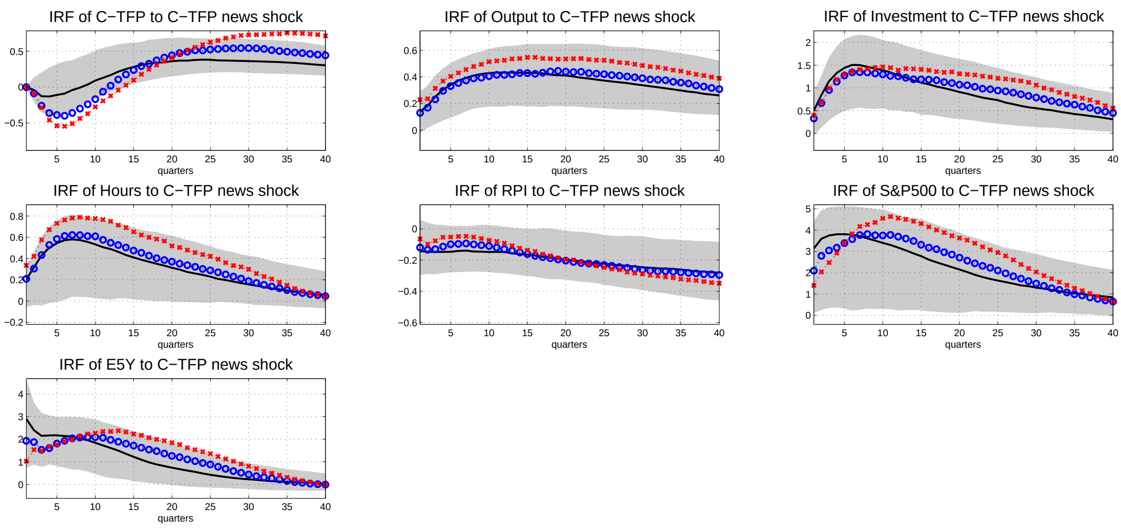

Figure 9: **Consumption specific TFP news shock, specification II.** Median responses to a consumption sector TFP news shock using three lag (black solid line), four lags (red line with crosses) and five lags (blue line with circles). The shaded gray areas are the 16% and 84% posterior bands generated from the posterior distribution of VAR parameters corresponding to the baseline identification with three lags. The units of the vertical axes are percentage deviations.

B.4 Forecast error variance decompositions

Figures 10, 11 and 12 show the forecast-error variance shares attributed to the variables in specification II in response to an aggregate-, investment sector- and consumption sector-TFP news shock. The aggregate TFP news shock as well as both of the two sectoral TFP news shocks explain a sizeable share of fluctuations in output and hours. This finding is consistent with findings in Görtz et al. (2016) who argue that TFP news shocks are important driving forces of business cycles.

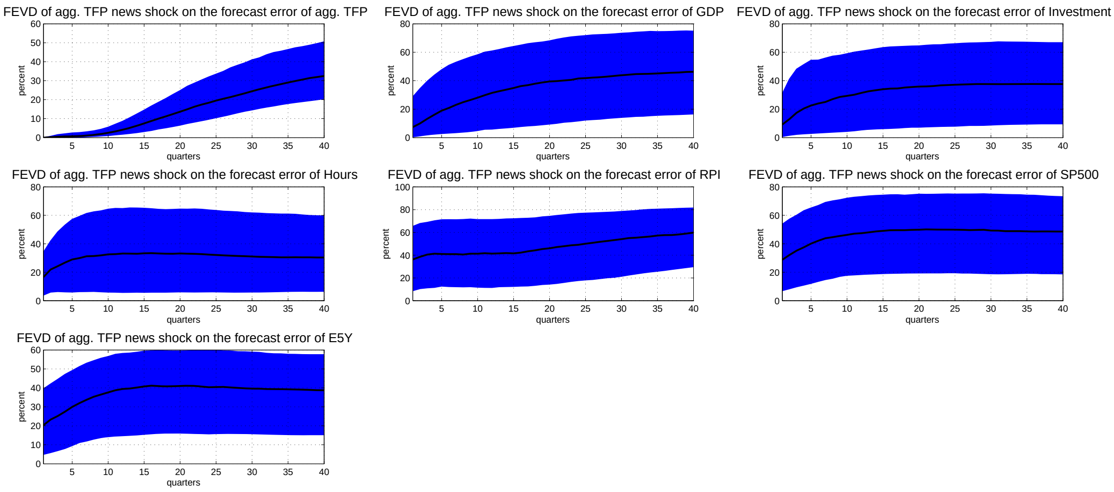

Figure 10: **Forecast error variance decomposition for the aggregate TFP news shock, specification II.** The median is shown by the solid line and the shaded gray areas are the 16% and 84% posterior bands generated from the posterior distribution of VAR parameters.

B.5 Extending the 7-variable VARs with sectoral TFP

As described in the main body of the paper, VAR specification II includes either a sectoral or aggregate TFP measure, one at a time. In this section, we extend this specification to an eight variable VAR by including both consumption and investment-specific TFP series. This allows us to evaluate how a TFP news shock in the one sector affects TFP in the other sector.

Figure 13 displays IRFs of the extended specification II to an investment-specific TFP news shock. It is notable that investment sector TFP increases significantly from about two years onwards while consumption sector TFP rises significantly with a considerable delay. Figure 14 displays responses to a consumption-specific TFP news shock when VAR specification II is extended to include both sectoral TFP measures. Similarly, this figure highlights that TFP in the investment sector rises before TFP in the consumption sector. It is interesting to note from this figure that

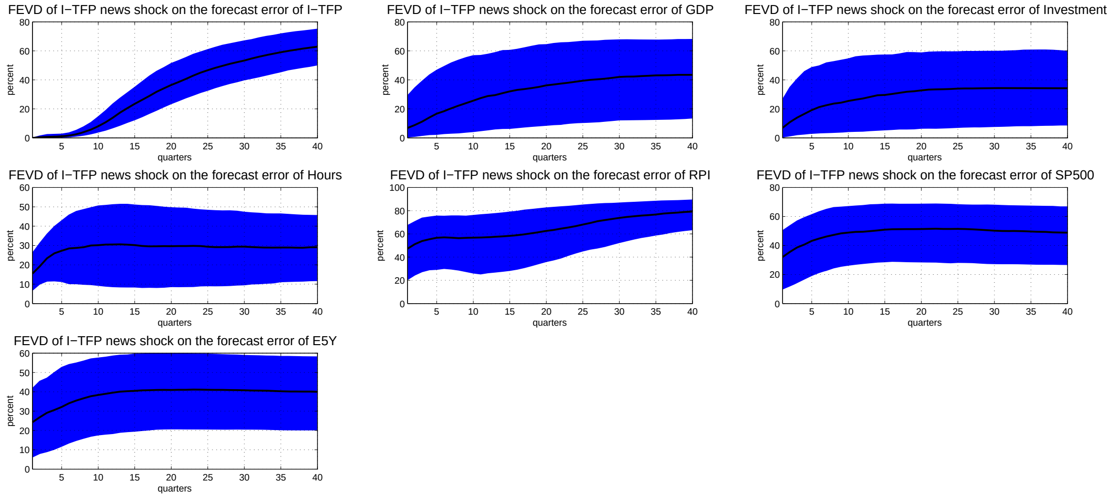

Figure 11: **Forecast error variance decomposition for the investment sector TFP news shock, specification II.** The median is shown by the solid line and the shaded gray areas are the 16% and 84% posterior bands generated from the posterior distribution of VAR parameters.

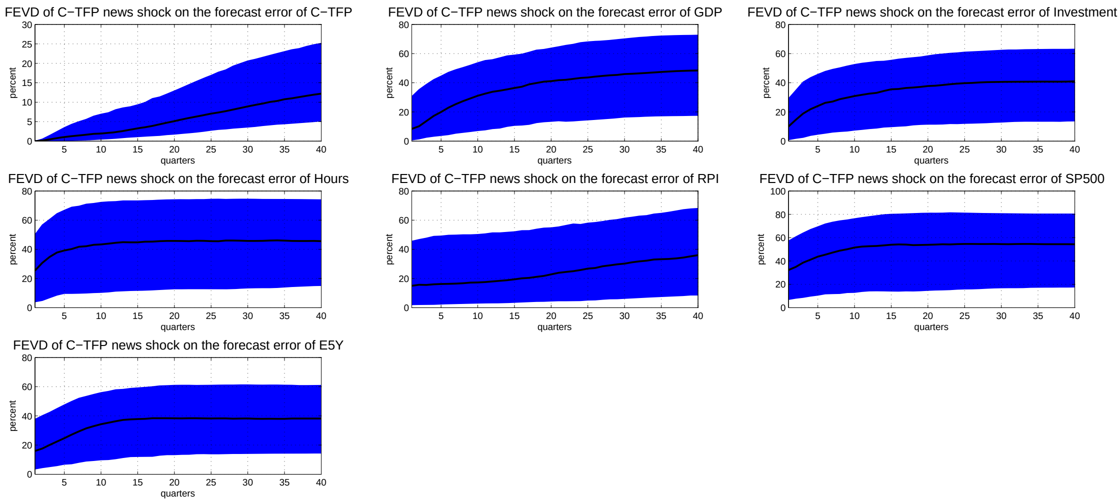

Figure 12: **Forecast error variance decomposition for the consumption sector TFP news shock, specification II.** The median is shown by the solid line and the shaded gray areas are the 16% and 84% posterior bands generated from the posterior distribution of VAR parameters.

the significant decline in the RPI occurs simultaneously with the significant increase of investment sector TFP. These observations further corroborate the results stated in the main body of paper on the diffusion of TFP news shocks from the investment to the consumption goods producing sector.

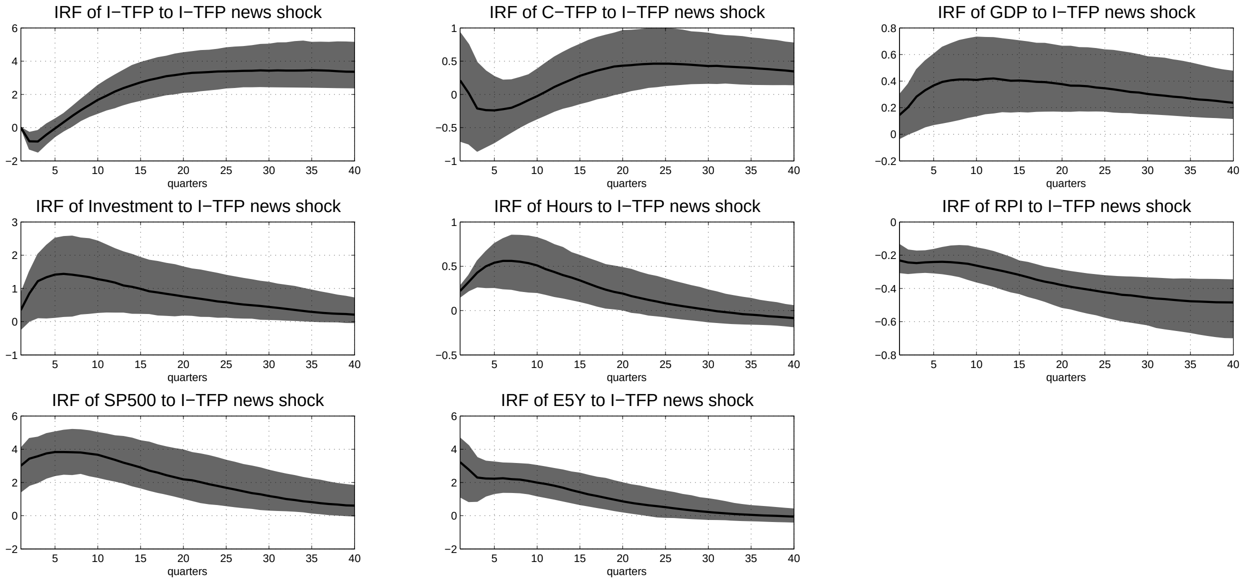

Figure 13: **Responses to an investment sector-specific TFP news shock. VAR specification II extended by consumption sector TFP.** Median responses to an investment-specific TFP news shock from an eight variable VAR (black solid line). The shaded gray areas are the 16% and 84% posterior bands. The units of the vertical axes are percentage deviations.

C Data Sources and Time Series Construction

Table 1 provides an overview of the data used to construct the observables. All the data transformations we have made in order to construct the dataset are described in detail below. As described in the main body, the VAR specifications are estimated with time series in levels.

Total Factor Productivity The data series for aggregate and sectoral utilization adjusted TFP are taken from John Fernald's website $(www.frbsf.org/economic-research/economists/jfernald/quarterly_{t}$ and are described in Fernald (2014). The construction of the TFP series is based on the growth accounting methodology in Basu et al. (2006) and corrects for unobserved capacity utilization. Throughout the paper we use the 2015 vintage which contains updated corrections on utilization from industry data following Basu et al. (2013).

Real and nominal variables. Consumption (in current prices) is defined as the sum of

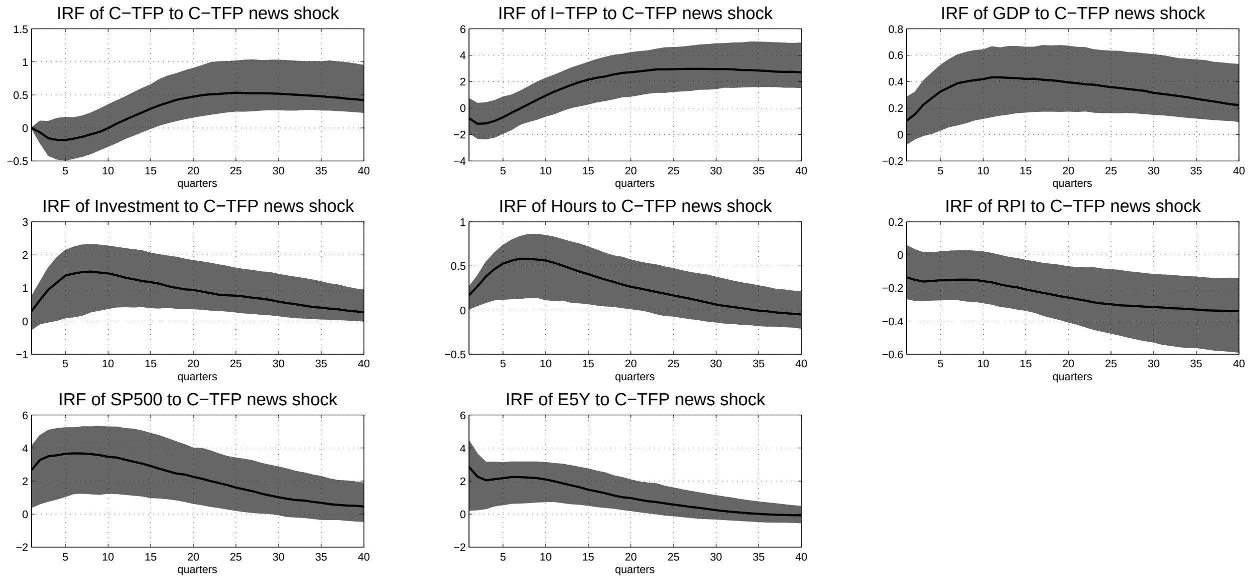

Figure 14: **Responses to a consumption sector-specific TFP news shock. VAR specification II extended by investment sector TFP.** Median responses to a consumption-specific TFP news shock from an eight variable VAR (black solid line). The shaded gray areas are the 16% and 84% posterior bands. The units of the vertical axes are percentage deviations.

personal consumption expenditures on services and personal consumption expenditures on non-durable goods. The times series for real consumption is constructed as follows. First, we compute the shares of services and non-durable goods in total (current price) consumption. Then, total real consumption growth is obtained as the chained weighted (using the nominal shares above) growth rate of real services and growth rate of real non-durable goods. Using the growth rate of real consumption we construct a series for real consumption using 2005 as the base year. The consumption deflator is calculated as the ratio of nominal over real consumption. We use the log change in the GDP deflator as our inflation measure, however results are nearly identical when we use the consumption deflator or CPI inflation. Analogously, we construct a time series for the investment deflator using series for (current price) personal consumption expenditures on durable goods and gross private domestic investment and chain weight to arrive at the real aggregate. The relative price of investment is the ratio of the investment deflator and the consumption deflator. Real output is GDP expressed in consumption units by dividing current price GDP with the consumption deflator.

Hours worked is given by hours of all persons in the non-farm business sector. All series described above are expressed in per capita terms using the series of non-institutional population, ages 16 and

Table 1: Time Series used to construct the dataset

Time Series Description	Units	Code	Source
Gross domestic product	CP, SA, billion \$	GDP	BEA
Gross Private Domestic Investment	CP, SA, billion \$	GPDI	BEA
Real Gross Private Domestic Investment	CVM, SA, billion \$	GPDIC1	BEA
Personal Consumption Exp.: Durable Goods	CP, SA, billion \$	PCDG	BEA
Real Personal Consumption Exp.: Durable Goods	CVM, SA, billion \$	PCDGCC96	BEA
Personal Consumption Expenditures: Services	CP, SA, billion \$	PCESV	BEA
Real Personal Consumption Expenditures: Services	CVM, SA, billion \$	PCESVC96	BEA
Personal Consumption Exp.: Nondurable Goods	CP, SA, billion \$	PCND	BEA
Real Personal Consumption Exp.: Nondurable Goods	CVM, SA, billion \$	PCNDGC96	BEA
Civilian Noninstitutional Population	NSA, 1000s	CNP160V	BLS
Non-farm Business Sector: Hours of All Persons	SA, Index 2005=100	HOANBS	BLS
S&P 500 Index			Robert Shiller
E5Y Confidence Indicator		Table 29	Michigan Survey
BAA corporate spread			St. Louis FED FRED

CP = current prices, CVM = chained volume measures (2005 Dollars), SA = seasonally adjusted, NSA = not seasonally adjusted. BEA = U.S. Department of Commerce: Bureau of Economic Analysis, BLS = U.S. Department of Labor: Bureau of Labor Statistics.

over.

Financial variables. The BAA spread is obtained from the Federal Reserve Bank of St. Louis online database FRED ($https : //fred.stlouisfed.org.$). The S&P 500 index is obtained from Robert Shiller's website ($http : //www.econ.yale.edu/\ shiller/data.htm$) and has been converted to a real per capita index by dividing with the consumption deflator and non-institutional population, ages 16 and over.

Survey data. The Michigan consumer confidence indicator data (E5Y) we use summarizes responses to the following question: "Looking ahead, which would you say is more likely – that in the country as a whole we'll have continuous good times during the next 5 years, or that we'll have periods of widespread unemployment or depression, or what?" The variable is constructed as the percentage giving a favorable answer minus the percentage giving an unfavorable answer plus 100.

References

Barsky, R. B. and Sims, E. R. (2011). News shocks and business cycles. *Journal of Monetary Economics*, 58(3):273–289.

Basu, S., Fernald, J., Fisher, J., and Kimball, M. (2013). Sector specific technical change. *Mimeo.*

Basu, S., Fernald, J., and Kimpball, M. (2006). Are technology improvements contractionary? *American Economic Review*, 96(5):1418–1448.

Fernald, J. (2014). A quarterly, utilization–adjusted series on total factor productivity. *Working Paper*, (2012-19).

Forni, M., Gambetti, L., and Sala, L. (2014). No news in business cycles. *Economic Journal*, 124:1168–1191.

Francis, N., Owyang, M., Roush, J., and DiCecio, R. (2014). A flexible finite-horizon alternative to long-run restrictions with an application to technology shocks. *Review of Economics and Statistics*, 96:638–647.

Görtz, C., Tsoukalas, J., and Zanetti, F. (2016). News shocks under financial frictions. *University of Glasgow Working Paper.*